Compact Description of 3D Image Gamut by Singular Value Decomposition

Hiroaki Kotera and Ryoichi Saito
Dept. Information and Image Sciences, Chiba University, Japan

Abstract

This paper proposes a compact description method for image gamut shell. 3D **I-DGMA** (Image-to-Device Gamut Mapping Algorithm) is an ideal way to map the display image to the inside of printer gamut. **I-DGMA** makes use of the relation between image and device gamut boundaries. The gamut shape data should be described in a compact format. In our proposal, it is given by a 2D array called r-image, which is measured as the maximum radius distance in polar angle. The r-image is compressed by SVD and the image gamut shell is reconstructed from the compact SVD parameters and used for I-D mapping.

Introduction

A variety of GMAs[1,2] are under developments. They are mostly designed to work in 2D L-C planes. So far, 3D GMA is not major but a few works have been reported.[3-5] Most of them characterize the devices gamut not the images, based on Device-to-Device (D-D), not I-D.[8] They don't reflect the image gamut exactly. A key factor to real 3D GMA is to extract the 3D image gamut from the random color distributions quickly and to describe its boundary. In the previous paper,[7] we proposed a Gamut Boundary Descriptor (GBD) by partitioning the color space into sub-spaces to include constant number of samples. However, this method can't be applied to the ***r-image*** description because of uneven division in polar angle. Here a constant division in discrete polar angle (θ, φ) is introduced to extract the image gamut surface. The GBD is desirable to be expressed as compact as possible, such as an analytical approach based on gamut kernel representation.[6] In this paper, gamut shell is described as the simple radial distances, ***r-image*** and we try to compress the GBD by applying DCT or SVD.

Extraction of Image Gamut

Letting the image color center be [L_0*, a_0*, b_0*] the radial distance is measured from the image center as

$$r_i = \left[\left(L_i^* - L_0^*\right)^2 + \left(a_i^* - a_0^*\right)^2 + \left(b_i^* - b_0^*\right)^2 \right]^{1/2} ;\ 1 \le i \le n \quad (1)$$

The polar angle of each pixel in CIELAB is defined by

$$\theta_i = \tan^{-1}\left[\frac{b_i^* - b_0^*}{a_i^* - a_0^*} \right] ;\ 0 \le \theta_i \le 2\pi \quad (2)$$

$$\varphi_i = (\pi/2) + \tan^{-1}\left(\frac{L_i^* - L_0^*}{\left\{ \left(a_i^* - a_0^*\right)^2 + \left(b_i^* - b_0^*\right)^2 \right\}^{1/2}} \right) ;\ 0 \le \varphi_i \le \pi \quad (3)$$

Here, the gamut surface is formed by picking up the points with the maximum radial distance in every segment divided by ($\Delta\theta$, $\Delta\varphi$) as shown in Fig.1.

$$\begin{aligned} &\boldsymbol{r} = [r_{jk}] = [\max\{r_i\}] \ ;\quad 1 \le i \le n \\ &\text{for } (j-1)\Delta\theta \le \theta_i \le j\Delta\theta \ \text{ and } \ (k-1)\Delta\varphi \le \varphi_i \le k\Delta\varphi \\ &\Delta\theta = 2\pi/M \ ;\ 1 \le j \le M \\ &\Delta\varphi = \pi/N \ ;\ 1 \le k \le N \end{aligned} \quad (4)$$

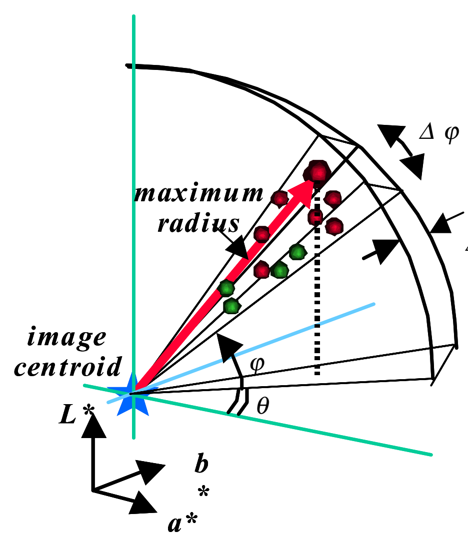

Figure 1. Segmentation of image gamut in Polar coordinate

Figure 2 (a) and (b) show the sRGB test image "bride" and its color map in CIELAB. The distribution of radial vectors [r_{jk}] is illustrated in (c) and the gamut shell is represented by connecting these radial points as given in (d). As well, the printer gamut shell is shaped from a color distribution of measured color chips.

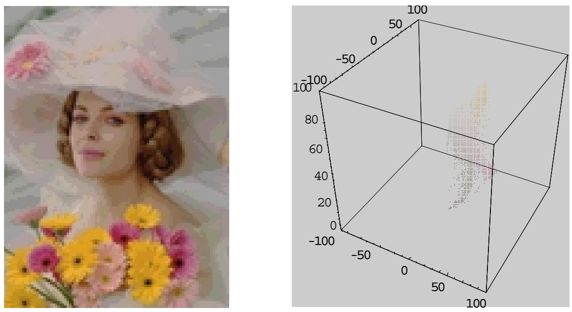

(a) image "wool" *(b) Color map in CIELAB*

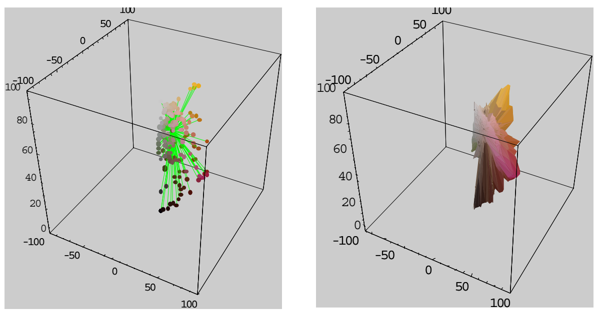

(c) Radial vectors to gamut surface *(d) Gamut shell*

Figure 2. Image gamut shell from radial vectors

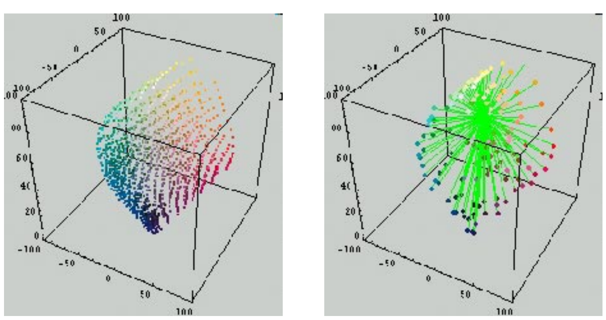

(a) Color distribution of Chips *(b) Radial vectors*

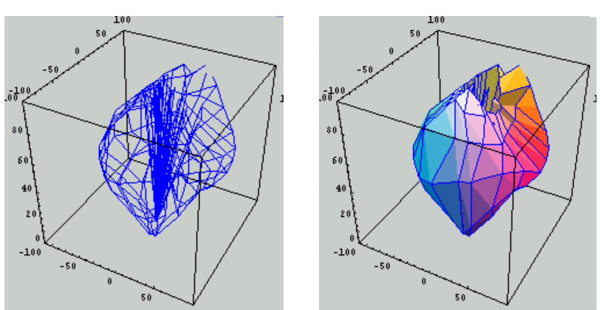

(c) Gamut shell in wire frame *(d) Gamut shell surface*

Figure 3. Formation of Device Gamut Shell (Inkjet printer)

The GBD for output device was examined for Epson PM800C inkjet photo prints. Figure 3 shows (a): color distribution of 11^3=1331 chips in CIELAB space, (b): radial vectors segmented in polar coordinate, (c): gamut shell shape represented by wire frame, and (d): gamut shell surface rendered by polygon, respectively.

r-Image and Compression

The ***r*-*image*** is a gray scale image given by $M \times N$ matrix $\boldsymbol{r}=[r_{jk}]$. If the gamut shell has a smooth 3D surface, the array r_{jk} will be highly correlated in spatial. The ***r*-*image*** can be compressed by applying orthogonal transform coding such as DCT.

Compression by DCT

The ***r*-*image*** is transformed into spatial frequency components $\boldsymbol{R}$ by forward $M \times M$ DCT.

$$\boldsymbol{R} = \left[R_{jk}\right] = \boldsymbol{A}^t \boldsymbol{r} \boldsymbol{A} \tag{5}$$

$$\boldsymbol{A} = \left[a_{jk}\right], \quad a_{jk} = \begin{cases} \dfrac{1}{\sqrt{M}}, & \text{for } k = 1 \\ \dfrac{2}{\sqrt{M}} \cos\left(\dfrac{(2j-1)(k-1)\pi}{2M}\right), & \text{for } k = 2, \cdots, M, \\ & j = 1, 2, \cdots, M \end{cases} \tag{6}$$

The inverse IDCT is given by the same formula

$$\boldsymbol{r} = \boldsymbol{A}\boldsymbol{R}\boldsymbol{A}^t \tag{7}$$

Since the spatial frequency energy is concentrated in low frequency components of $\boldsymbol{R}$, the ***r*-*image*** is approximately reconstructed from the reduced $m \times m$ ($m<M$) matrix by

$$\hat{\boldsymbol{r}} \cong \boldsymbol{A}\boldsymbol{R}^m \boldsymbol{A}^t, \quad \boldsymbol{R}^m = \left[R_{jk}^m\right], \quad R_{jk}^m = \begin{cases} R_{jk}, & \text{for } j, k \le m \\ 0 & \text{for } j, k > m \end{cases} \tag{8}$$

Compression by SVD

DCT is easy to use because its basis function is prefixed independent of image. However, the image has its own shell shape, then the image-dependent basis function may be better for the gamut description. Here SVD has been tested.

The ***r*-*image*** can be expressed by SVD as

$$\boldsymbol{r} = \left[r_{jk}\right] = \boldsymbol{U}\boldsymbol{\Lambda}\boldsymbol{V}^t \tag{9}$$

where, the columns of $\boldsymbol{U}$ and $\boldsymbol{V}$ are the eigenvectors of $\boldsymbol{r}\boldsymbol{r}^t$ and $\boldsymbol{r}^t\boldsymbol{r}$, and $\boldsymbol{\Lambda}$ is the diagonal matrix containing the singular values of $\boldsymbol{r}$ along its diagonal.

Because $\boldsymbol{U}$ and $\boldsymbol{V}$ are orthogonal, $\boldsymbol{\Lambda}$ is expressed by

$$\boldsymbol{\Lambda} = \boldsymbol{U}^t \boldsymbol{r} \boldsymbol{V} = \begin{bmatrix} \lambda_1 & 0 & \cdots\cdots & 0 \\ 0 & \lambda_2 & 0 \cdots\cdots & 0 \\ \vdots & & & \vdots \\ \vdots & & \ddots & \vdots \\ 0 & \cdots\cdots & 0 & \lambda_M \end{bmatrix} \tag{10}$$

The ***r**-image* is approximately restored from the reduced numbers of singular values and eigenvectors as,

$$\hat{\boldsymbol{r}} = \left[\hat{r}_{jk}\right] \cong \boldsymbol{U}_m \boldsymbol{\Lambda}_m \boldsymbol{V}_m^t \tag{11}$$

The matrix $\boldsymbol{r}$ can be restored from m ($< M$) singular values and the corresponding vectors of $\boldsymbol{U}$ and $\boldsymbol{V}$.

$$\boldsymbol{\Lambda}_m = \begin{bmatrix} \lambda_1 & 0 & \cdots\cdots & 0 \\ 0 & \lambda_2 & 0 \cdots & 0 \\ \vdots & & \ddots & \vdots \\ 0 & \cdots\cdots\cdots & & \lambda_m \end{bmatrix} \tag{12}$$

Reconstruction of Gamut Shell

The [L^*, a^*, b^*] value of ***r**-image* is recovered from the de-compressed $\hat{r}_{jk}$ values as

$$\hat{a}^*{}_{jk} \cong \hat{r}_{jk} \cos(j-0.5)\Delta\theta \sin(k-0.5)\Delta\varphi + a^*{}_0$$
$$\hat{b}^*{}_{jk} \cong \hat{r}_{jk} \sin(j-0.5)\Delta\theta \sin(k-0.5)\Delta\varphi + b^*{}_0$$
$$\hat{L}^*{}_{jk} \cong L_0^* - \hat{r}_{jk}\cos(k-0.5)\Delta\varphi \tag{13}$$

The RGB surface colors are also recovered from these [L*, a*, b*] values. Thus we can reconstruct the polygonal image gamut shell from discrete $\hat{r}$*-image* by rendering with these surface colors.

Experimental Results

Gamut Shell Representation by *r-image*

The compact description of image gamut shell was tested by DCT and SVD transform of r-image. Fig.4 (a) and (b) show the sRGB test image "wool" and its color map. Fig. (c) and (d) are its radial vector and the gamut shell rendered by polygon. Fig.4 (e) shows the r-image represented by 2D gray levels, where the magnitudes of radial vectors are arranged in (θ, φ) directions segmented by 32 × 32 discrete angles and (f) shows the corresponding surface colors located at the most outside points with the maximum radius.

Reconstruction from Reduced DCT and SVD Matrices

The ***r**-image* is approximately restored from the reduced number of DCT coefficients or SVD parameters. Fig.5 and Fig.6 show a comparison of reconstructed ***r**-image* and its gamut shell shape for image "wool" using the reduced dimensions of DCT and SVD matrices. The ***r**-image* reproduced by 4 × 4 DCT coefficients looks too much blurred just as low-pass filtered and its gamut shell shape obviously loses its details due to the lack of higher spatial frequency components as shown in (a). They were still insufficient even by 8 × 8 DCT as shown in (c).

On the contrary, the ***r**-image* and the gamut shell shape in Fig. 5 (b) were very well recovered by 4 × 4 SVD. The results in (d) by 8 × 8 SVD were restored in more details as compared with the original in (g) by full 32 × 32 dimensions.

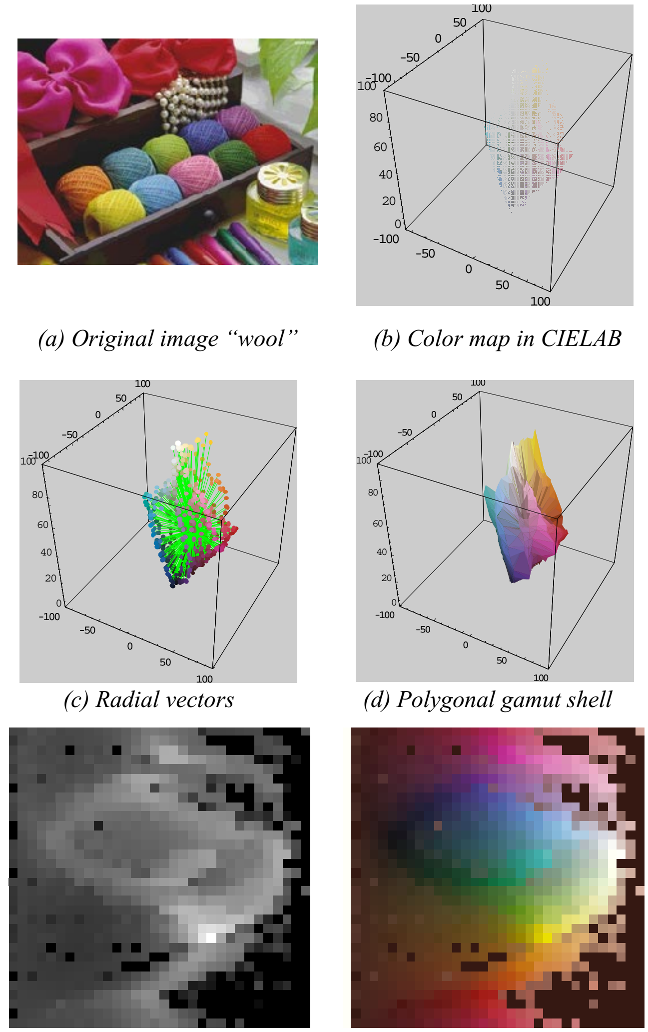

(a) Original image "wool" *(b) Color map in CIELAB*

(c) Radial vectors *(d) Polygonal gamut shell*

(e) **r**-image *by gray levels* *(f) Shell surface color*

*Figure 4. Test image and its gamut shell by **r**-image*

Figure 5(f) and Figure 6(f) by 16 × 16 SVD give the almost perfect reconstructions in the spatial resolution of ***r**-image* and in the complex shell shape.

Singular Values Distribution and Eigen Vectors

The ***r**-image* is decomposed by orthogonal eigen vectors $\boldsymbol{U}$ and $\boldsymbol{V}$ through the singular value $\boldsymbol{\Lambda}$. The energy of ***r**-image* is mostly concentrated to the lower order of eigen vectors as weighted by $\boldsymbol{\Lambda}$. Figure 7(a) and (b) show the 3D profile of matrix $\boldsymbol{U}$ and the first four eigen vectors for image "wool". As well, those of matrix $\boldsymbol{V}$ are shown in Fig. 7(c) and (d).

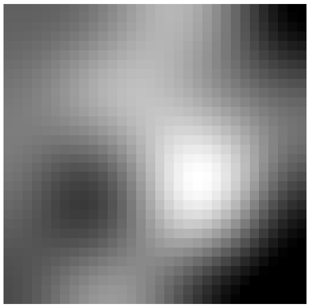

(a) 4 x 4 DCT

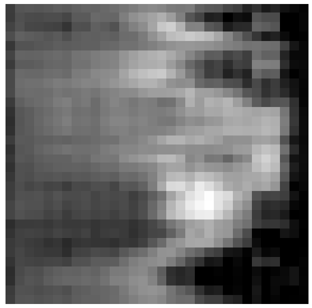

(b) 4 x 4 SVD

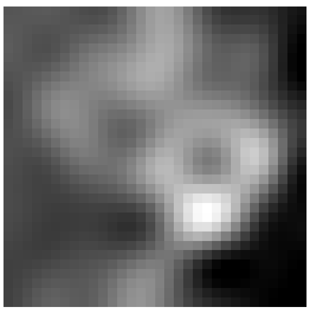

(c) 8 x 8 DCT

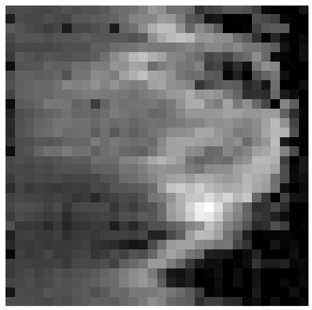

(d) 8 x 8 SVD

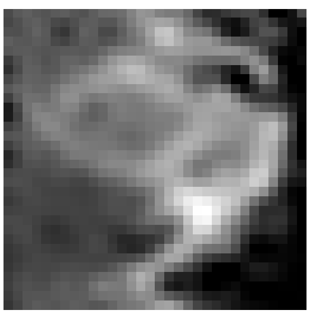

(e) 16 x 16 DCT

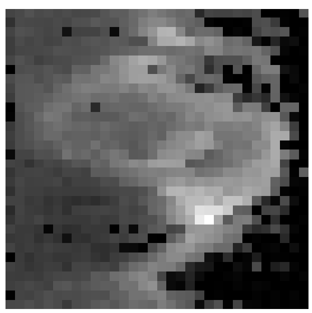

(f) 16 x 16 SVD

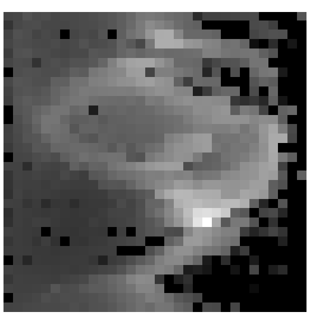

(g) Original ***r****-image (32 x 32)*

Figure 5. ***r****-images reconstructed from reduced DCT and SVD matrices for image "wool"*

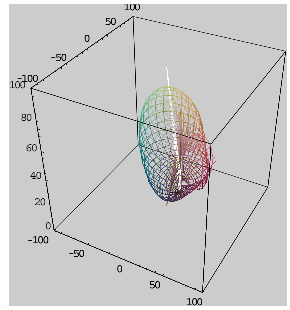

(a) 4 x 4 DCT

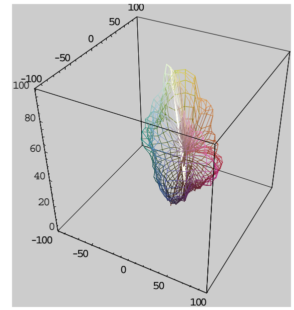

(b) 4 x 4 SVD

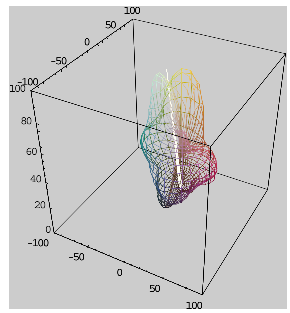

(c) 8 x 8 DCT

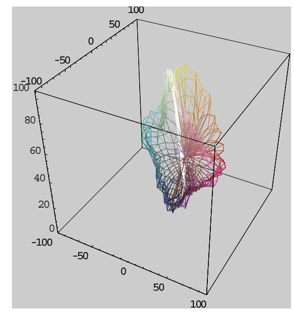

(d) 8 x 8 SVD

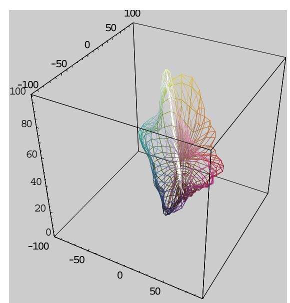

(e) 16 x 16 DCT

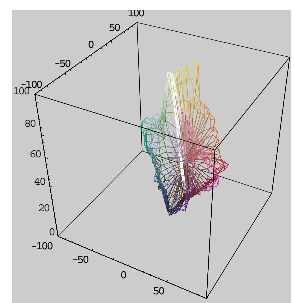

(f) 16 x 16 SVD

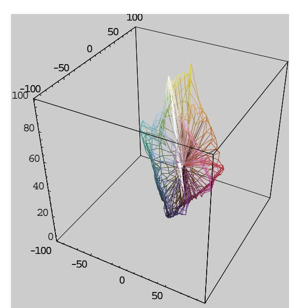

(g) Original wire-frame gamut shell

Figure 6. Gamut shell shapes reconstructed from reduced DCT and SVD matrices for image "wool"

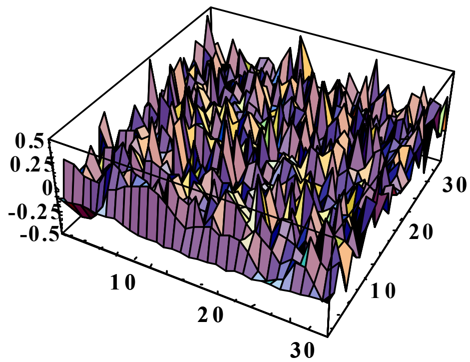

*(a) Profile of eigen vectors matrix **U***

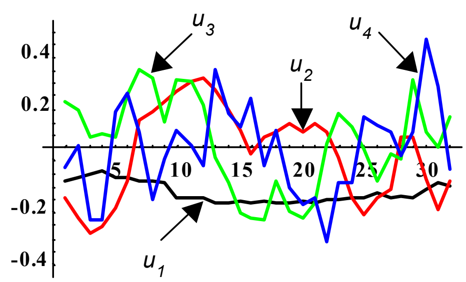

*(b) First four eigen vectors of matrix **U***

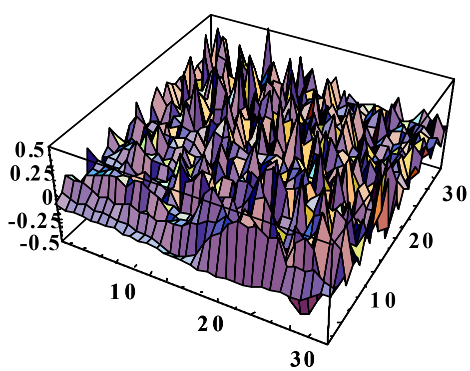

*(c) Profile of eigen vectors matrix **V***

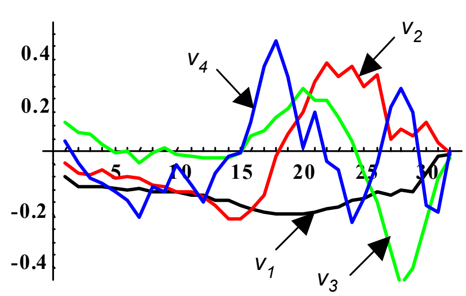

(d) First four eigen vectors of matrix V

Figure 7. Eigen vectors for image "wool"

Figure 8 shows how the singular values $\boldsymbol{\Lambda}=[\lambda_i]$ drop off rapidly in magnitude for the four different sRGB test images. The singular values are mostly concentrated in the lower orders less than 4 or 5. Surely both the ***r**-image* and gamut shell shape were almost well reconstructed by the products of first four row vectors of ***U***, four singular values and four column vectors of ***V*** as shown in Fig.5 and Fig.6.

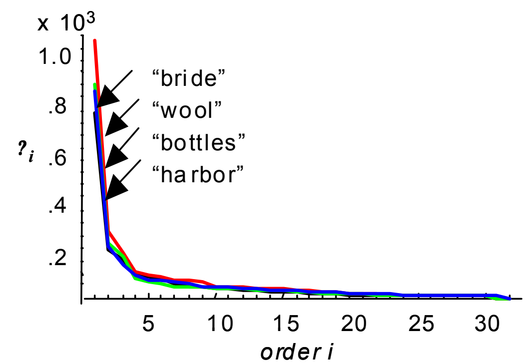

Figure 8. Distribution of singular values in four images

Reconstruction Error

The reconstruction error in gamut shell was measured by color differences in the reproduction of surface colors. The [*L*, a*, b**] values on the gamut surface are restored from the reconstructed ***r**-image* using Equ. (13). Fig. 9 shows the color differences in ΔE^*_{94}(rms) for the gamut surface colors reconstructed from the reduced dimensions of inverse DCT and inverse SVD. Reconstruction error ΔE^*_{94}(rms) in "bride" was 1.51 for 4 × 4 DCT and 0.93 for 8 × 8 DCT, while it was reduced to 1.01 for 4 × 4 SVD and 0.66 for 8 × 8 SVD. These figures include the minimum quantization error by discrete polar angle segmentation. For example, minimum ΔE^*_{94}(rms) was calculated as 0.34 for 32 × 32 divisions in (θ, φ) angles. These reconstruction errors look to be small when measured by ΔE^*_{94}(rms), because almost all the gamut surface colors are highly saturated and ΔE^*_{94} value is discounted for the higher saturation as compared with ΔE^*_{ab}. The color differences in ΔE^*_{ab}(rms) were accounted as 4 or 5 times larger than ΔE^*_{94}(rms) in the case of Fig. 9.

Discussion and Conclusion

The image gamut shell shape was simply represented by a set of radial vectors, ***r**-image* in segmented polar angles. The ***r**-image* could be compactly approximated with small number of singular values by SVD. The radial vector's segmentation around 32 × 32 in (θ, φ) angles gives accurate reconstruction of gamut shell shapes, if the ***r**-image* is compressed by SVD using four or more eigen values. Although the transform matrix ***A*** of DCT is fixed independent of image, the eigenvectors ***U*** and ***V*** in SVD should be computed and transmitted by every image.

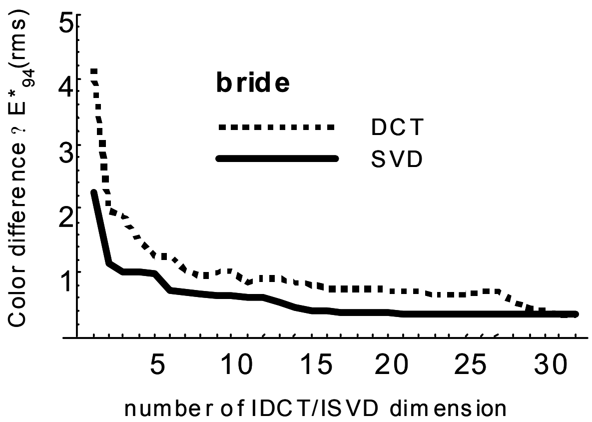

(a) ΔE94 (rms) error: ***bride***

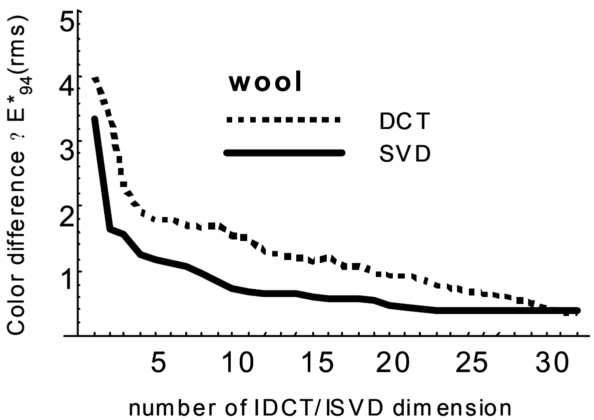

(b) ΔE94 (rms) error: ***bottle***

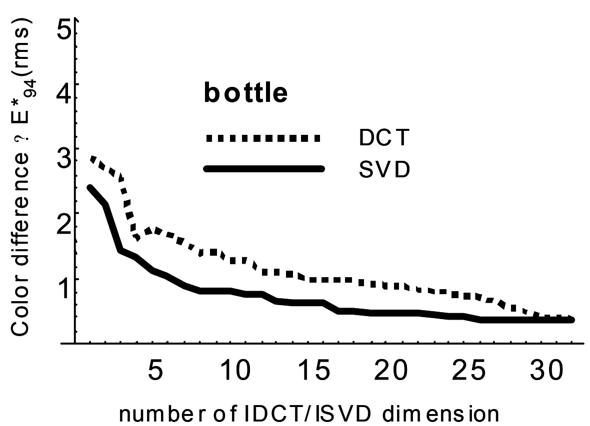

(c) ΔE94 (rms) error: ***wool***

Figue 9. Reconstruction error in gamut surface colors

Because the ***r**-image* is a gray scale image and highly correlated spatially, it may be further more compressed by applying conventional picture coding method such as JPEG2000. Future works will be continued focusing on the more compact description of gamut shell shapes with smoothed rendition of 3D surface.

Acknowledgement

This work has been supported by Research Project Grant-in-Aid for Scientific of Research No.12650363 of Japan.

References

1. J. Morovic and M. R. Luo, The Fundamentals of Gamut Mapping: A survey, *J. IS&T*, **45**, 3, pp.283-290 (2001)
2. L. W. MacDonald and M. R. Luo, *Color Imaging*, John Wiley & Sons (1999)
3. K. E. Spaulding et al, Ultra Color; A new gamut mapping strategy, *Proc. SPIE,* **2414**, 61-68 (1995).
4. N. Katoh et al, Three-dimensional gamut mapping using various color difference formulae and color spaces, *J. E. I.*, **8**(4), p. 365-379 (1999).
5. Chen Hung-Shing and H. Kotera, Three-dimensional Gamut Mapping Method Based on the Concept of Image-dependence, *Proc. IS&T's NIP16*, p.783-786 (2000).
6. P. G. Herzog, Analytical Color Gamut Representation, *J. IS&T*, **40,** 3, pp.516-521 (1996).
7. R. Saito, and H. Kotera, Extraction of Image Gamut Surface and Calculation of its Volume, *Proc. 8th CIC*, p. (2000).
8. Chen Hung-Shing, M. Omamiuda and H. Kotera, Gamma-Compression Gamut Mapping Method Based on the Concept of Image-to-Device, *J. IS&T*, **45,** 2, pp.141-151 (2000).
9. Chen Hung-Shing, M. Omamiuda and H. Kotera, Three-dimensional Gamut Mapping Method Based on the Concept of Image-dependence, *J. IS&T*, to be published (2001)

Biography

Hiroaki Kotera received his B.S degree from Nagoya Institute of Technology and Doctorate from University of Tokyo. He joined Matsushita Electric Industrial Co in 1963. Since 1973, he has been working in digital color image processing at Matsushita Research Institute Tokyo, Inc. In 1996, he moved to Chiba University. He is a professor at Dept of Information and Image Sciences. He received Johann Gutenberg prize from SID in 1995 and journal awards from IS&T in 1993, from IIEEJ in 1990 and 2000.